# Microstructure and Microhardness Characterization of $Cr_3C_2$-SiC Coatings Produced by the Plasma Transferred Arc Method

*Serkan Islak, Özkan Eski, Kastamonu, Soner Buytoz, Elazig, Muzaffer Karagöz, Bartin, Turkey, and Joseph Stokes, Dublin, Ireland*

The purpose of this work was to investigate the coatings made of $Cr_3C_2$ and SiC powder manufactured on AISI 304 stainless steel applied by the plasma transferred arc (PTA) welding process. SiC content in the produced coated layer was varied between 0-100 wt.% and the effect of SiC concentration on the microstructure and hardness of the coating was measured experimentally. SEM analyses revealed that the composite coatings had a homogeneous, nonporous, and crack-free microstructure. Dendrites and interdendrite eutectics formed on the coating layer, subject to the temperature gradient and the solidification ratio. There was a significant increase in the hardness of coating layers with the effect of the γ-(Fe,Ni), $Cr_7C_3$, $Cr_{23}C_6$, $Fe_5C_2$, $Cr_3Si$, $CrSi_2$, $Fe_{0.64}Ni_{0.36}$, $CFe_{15.1}$, C-(Fe,Cr)-Si phases formed in the microstructure. In comparison to the substrate, the microhardness of the coatings produced by PTA were 2.5-3.5 times harder.

Metallic materials are often subject to surface modifications to enhance their functionability against wear, corrosion, and fatigue, factors they are exposed to under working conditions. This is the reason why such procedures have become the focal point for researchers [1, 2]. In addition, to conventional heat-treatment, surface modification procedures include surface coating techniques, where a layer, harder than that of the substrate, often with different chemical composition to the substrate, is formed. The difference between these surface coating techniques and other thermal spraying – ion sourced coating and vapour deposition coatings – is that the coating layer is connected to the substrate with a strong metallurgical bond. As a result laser-based and plasma-based coating technologies are rapidly progressing. However, the laser technology used in the surface coating industry is expensive and its productivity is low, which limits its usage in the manufacturing environment. Recently, the plasma transferred arc welding technique (PTA) has been used more actively as it is cost-efficient and it yields high performance [3]. The PTA coating method has numerous advantages, e.g. excellent arc stability, low heat distortion in components, high process speed (~2-16 mm/s), high energy density, and low energy input ($10^5$-$10^6$ $Wcm^{-2}$) [4, 5].

In PTA hardfacing, the metallic powder placed on the substrate is melted using a plasma arc. Fusion is created in the substrate in order to form a strong metallurgical bond between the coating layer and the substrate [6-8]. This technique is applied to industry parts such as valves, glass moulds, extruders, pumps and turbine parts, extrusion moulds for brick and tile, hot processing tools, drilling equipment, mining equipment, hydraulic cylinders, etc. [9, 10].

Carbide-based powders are added to the matrix powder in order to improve the surface properties of the metals during the surface coating formation. $Cr_3C_2$ and SiC are preferred for coating applications as they contribute to increased wear and corrosion resistance due to their high melting points and high hardness values [11, 12]. In a study conducted by Dawei et al. [13] they formed $Cr_3C_2$ particle reinforced (percentage of weight of 50 %) Ni-based composites on the surface of AISI 1045 steel, using a $CO_2$ laser system. The fundamental factors that enable the composite coating to gain strength were undissolved $Cr_3C_2$ particles in the nickel matrix, the high number of dendrites formed enclosed by fine eutectics, and the sedimentation of $Cr_7C_3$, $Fe_{23}(C,B)_6$ compounds during the solidification of the composite coating.

Numerous studies regarding PTA coatings are available in literature. Sudha et al. [14] studied the microstructural properties of AISI 304 stainless steel by coating its surface with Ni-Cr-B-Si alloy powders, using the plasma transferred arc method.

*Table 1. The substrate and the chemical composition of the coating powders used in the coating process*

| | | Substrate & powders | | |
|---|---|---|---|---|
| | | AISI 304 steel | $Cr_3C_2$ powder | SiC powder |
| Composition (wt.-%) | C | 0.035 | 24.07 | 27.65 |
| | Mn | 1.24 | – | – |
| | Si | 0.40 | – | 72.35 |
| | Ni | 8.73 | – | – |
| | Cr | 18.57 | 75.93 | – |
| | Fe | balance | – | – |

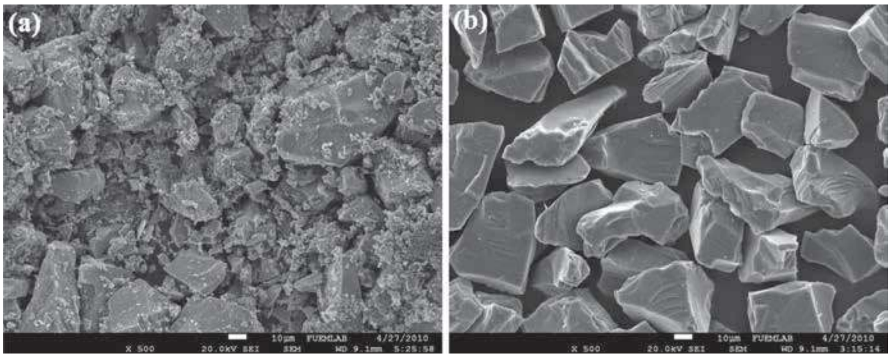


*Figure 1. SEM images of the powders used in the coating process, a) $Cr_3C_2$, b) SiC*

*Table 2. PTA coatings and production parameters*

| Sample number | Mixture of coating powders | Production parameters | |
|---|---|---|---|
| | | electrode diameter (mm) | 4.6 |
| | | shielding gas flow rate, Ar (l/min) | 15 |
| 1 | 100 wt.-% $Cr_3C_2$ | plasma gas flow rate, Ar (l/min) | 0.2 |
| 2 | 75 wt.-% $Cr_3C_2$ – 25 wt.-% SiC | current (A) | 150 |
| 3 | 50 wt.-% $Cr_3C_2$ – 50 wt.-% SiC | voltage (V) | 20 |
| 4 | 100 wt.% SiC | production speed (mm/s) | 2.2 |

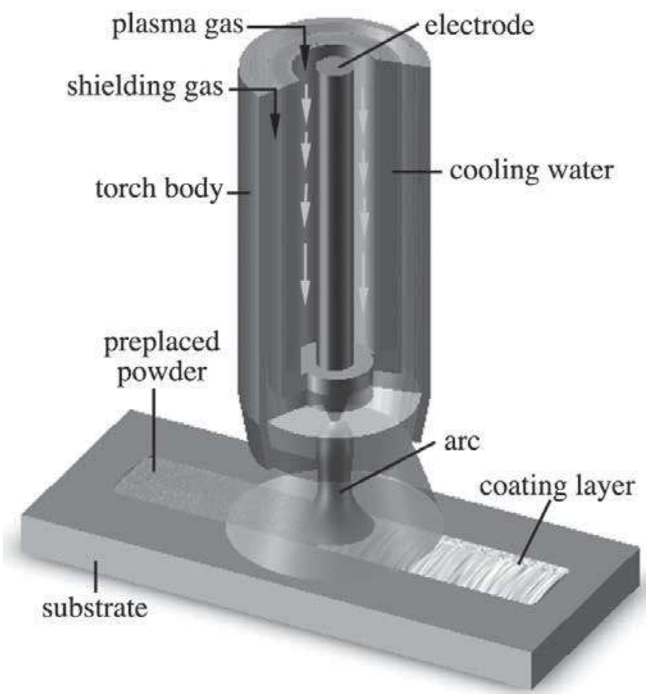


*Figure 2. Schematic illustration of PTA weld-surfacing process*

Apart from the γ-Ni solid solution the researcher observed primary phase $Cr_2B$, $Cr_7C_3$, and $Cr_3C_2$ carbides as well as borides in the microstructure. They established that the coating hardness of the solid phases in the structure reached 700 HV. The $Cr_7C_3$ distributed within the matrix increased the wear resistance and hardness of the coating layer. Huang et al. [15] coated the surface of low carbon steel with a Ni-based alloy + 30 % $Cr_3C_2$ composite powder mixture, using plasma transferred arc welding. This research established that the microstructure of the coating changed from a hypoeutectic structure to a hypereutectic structure with the addition of $Cr_3C_2$, and that the levels of hardness and wear resistance were higher than that of the $Cr_3C_2$ free coating. Buytoz and Ulutan [16] coated the surface of AISI 304 stainless steel with various amounts of SiC powder, using gas tungsten arc welding (GTAW). They established that primary phase $M_7C_3$ carbides formed in the microstructure, and the hardness of the coating layer changed from 890 HV and 1210 HV, because of these carbides. Guo et al. [17] coated the surface of low carbon steel with SiC powder containing various fine and coarse particles, using the plasma melt injection process. The hardness and wear resistance of the coating increased in comparison to the substrate. They established that the wear resistance of the coating formed using coarse SiC particles was higher in comparison to the coating formed using fine SiC particles. Thawari et al. [18] coated the surface of medium carbon steel with SiC powder by laser surface alloying process. $Fe_7C_3$, $Fe_3C$, $Fe_3Si$, and $Fe_2Si$ phases were formed in the microstructure, and the wear resistance of the coating was excellent in comparison to the substrate.

In this study, $Cr_3C_2$ + SiC composite coatings were formed on the surface of AISI 304 stainless steel by plasma transferred arc (PTA) coating method. Scanning electron microscope (SEM), X-ray diffractometer (XRD), and energy dispersive spectroscopy (EDS) were used to for characterization of the microstructure and chemical composition of the coating. The change in microstructure and hardness was analyzed by adding various amounts of SiC powder to $Cr_3C_2$ powder.

## Experimental

100 mm × 20 mm × 10 mm AISI 304 stainless steel was used as substrate material in the surface coating process. The surfaces of

specimens were air blasted to remove stains and other contaminants from their surface, then rinsed with acetone, prior to plasma transferred arc coating. $Cr_3C_2$ and SiC powders, whose chemical compositions are illustrated in Table 1, were used as coating powders.

Figure 1 illustrates SEM images for each powder. Both coating powders were produced with gas atomisation and had a sharp-edged morphology. The grain size for $Cr_3C_2$ was -70+5 µm, and for SiC was -60+15 µm, respectively. The mixed powders were pasted onto the surface of the specimens using a small amount of alcohol in order to keep powders on the surface under the flow of argon during the PTA surfacing. Then, the alcohol containing powder mixtures were dried at 50 °C for 1 h. Table 2 summarizes the PTA coatings and the production parameters. Figure 2 illustrates the schematic diagram of the PTA weld-surfacing process.

The deposited specimens prior to metallographic examination preparation were first cut perpendicular to the coating surface. For microstrukture studies the cross-sections of coatings were polished using mechanical procedures, and were electrolytically etched using a 50 % $HNO_3$ + 50 % alcohol solution. The microstructures of the clad coating were examined by scanning electron microscopy (JEM-2100F, JEOL, Japan) with X-ray energy dispersion (EDS) attachment, which was used to analyze the chemical composition of the clad coating. The phases in the clad coating were analyzed using an X-ray diffractometer (Bruker AXS D8 Advanced System, Germany). A microhardness device (Future-Tech FM 700, Japan) with a testing load of 1.96 N was used to measure the hardness, along a line from the coating layer towards the substrate at 250 µm intervals with a loading time of 10 s.

## Results and Discussion

Figure 3 illustrates the XRD patterns of the $Cr_3C_2$ + SiC coating, produced by PTA. The microstructure of coatings produced on the surface of the AISI 304 stainless steel are formed from the phases γ-(Fe,Ni), $Cr_7C_3$, $Cr_{23}C_6$, $Fe_5C_2$, $Cr_3Si$, $CrSi_2$, $Fe_{0.64}Ni_{0.36}$, $CFe_{15.1}$, and C-(Fe,Cr)-Si. SiC and $Cr_3C_2$ peaks were not identified in the XRD patterns. This suggests that the coating powders dissolved completely in the melt pool.

Figures 4 to 11 illustrate the SEM microstructures of PTA coatings, which were crack-free. There is a planar structure

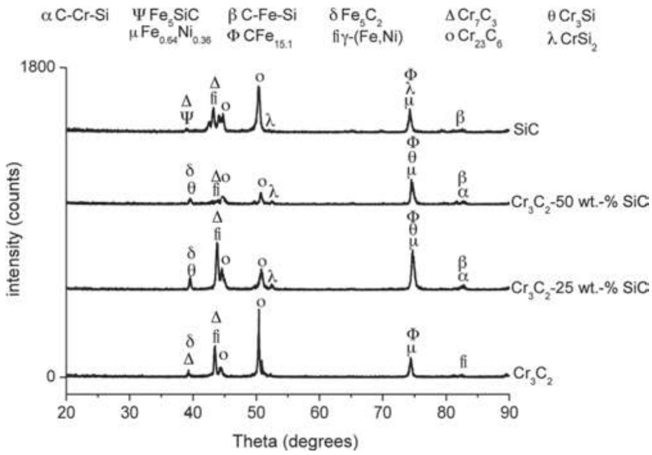


*Figure 3. XRD patterns of $Cr_3C_2$ and SiC coatings produced by PTA*

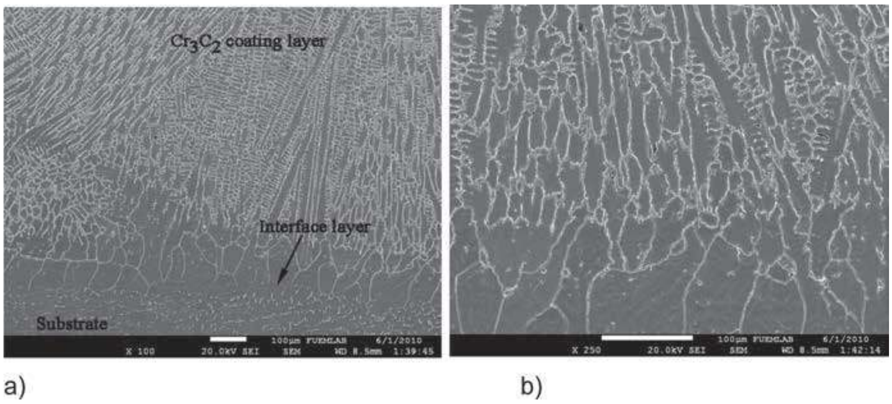


*Figure 4. SEM images of sample 1*

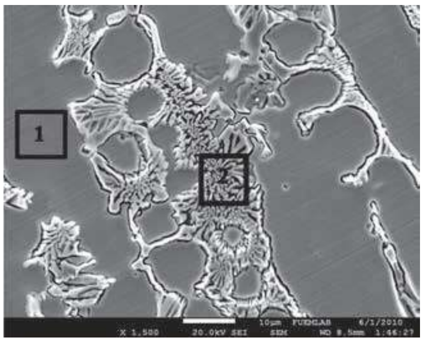


*Figure 5. SEM image of points 1 and 2 on coating 1*

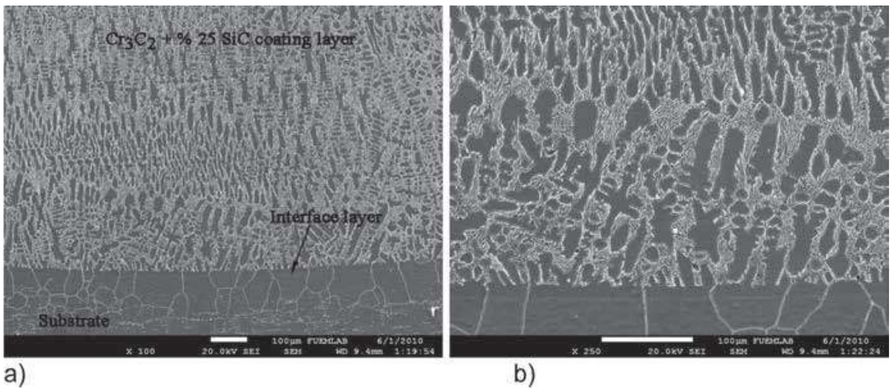


*Figure 6. SEM images of sample 2*

found at the interface (Figure 4a). Processing towards the coating surface, in order, with a cellular structure and dendrites with a columnar structure in various directions (Figure 4b). The structural change is associated with the solidification rate (R) of the metallic liquid in the PTA melt pool, and the temperature gradient (G) [15]. The G/R ratio of the interface between the coating layer and the substrate, whose temperature gradient is high and its solidification rate low, is significantly high. Hence, the interface displays a planar structure. Due to the fact that the interface has a planar structure, the metallurgical bonding between the substrate and the coating layer is ideal. The solidification rate increases rapidly after planar solidification, and the temperature gradient that was at its maximum value at the beginning, starts to decrease rapidly. In conclusion, the G/R ratio decreases causing the formation of a cellular structure. Dendritic solidification occurs after cellular solidification. The direction and dimensions of the dendrites vary in regions near the surface [19-21]. The convection and Marangoni effect of the protective atmosphere, during the coating process, causes the dendrites to solidify in random directions [18, 22]. Figures 4a, 6a, 8a, and 10a illustrate the change in the microstructure subject to the temperature gradient and solidification ratio (G/R).

The EDS analysis of 100 wt.-% $Cr_3C_2$ based coating was taken of points 1 and 2 as illustrated in Figure 5. Table 3 displays the results of EDS analyses. Dendrites and interdendrite eutectics were established throughout the microstructure. The $Cr_3C_2$ in the coating layer produced from 100 % $Cr_3C_2$ metallic powder by PTA was totally dissolved. Table 3 illustrates the chemical

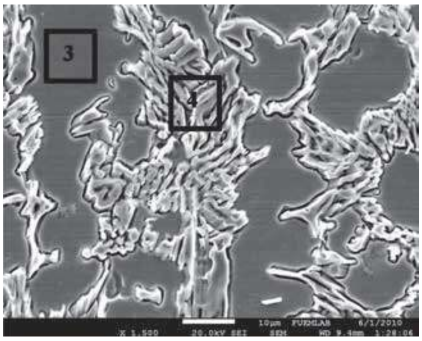


*Figure 7. SEM image of points 3 and 4 on coating 2*

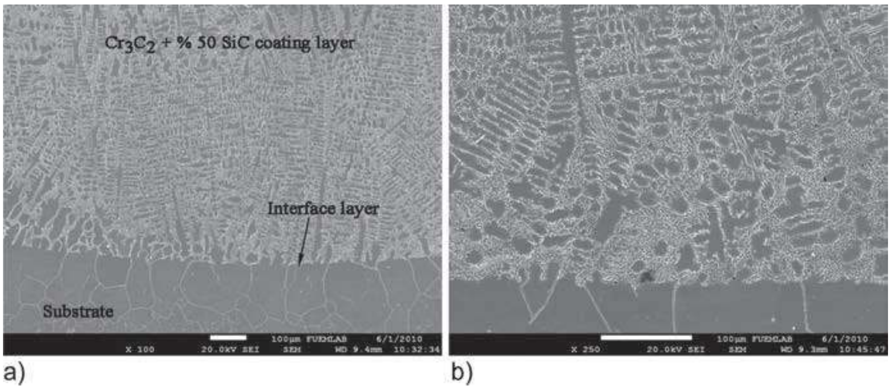


*Figure 8. SEM images of sample 3*

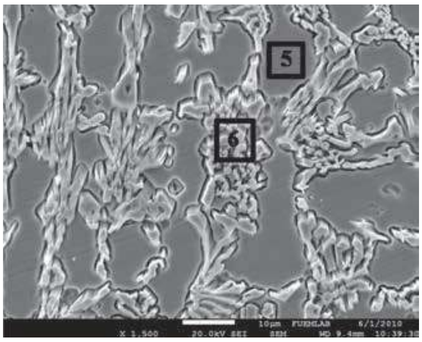


*Figure 9. SEM image of points 5 and 6 on coating 3*

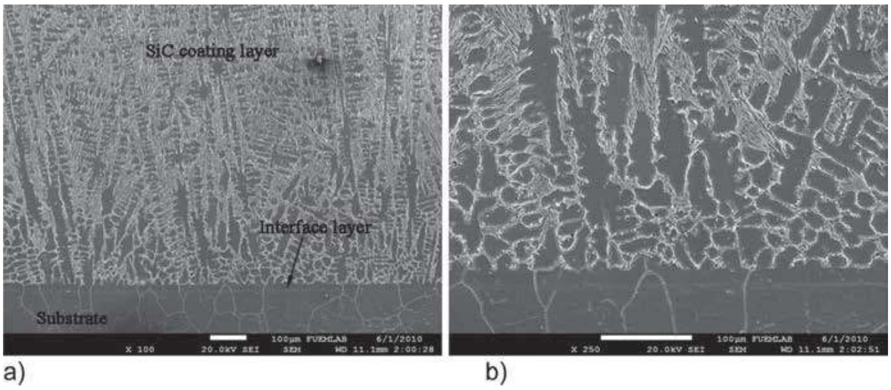


*Figure 10. SEM images of sample 4*

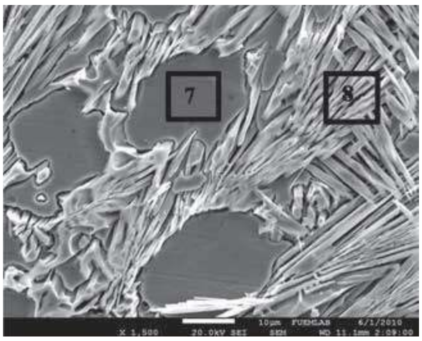


*Figure 11. SEM image of points 7 and 8 on coating 4*

*Table 3. EDS analysis at points 1 and 2 on coating 1*

| Phases | Chemical composition (wt.-%) | | | | |
|---|---|---|---|---|---|
| | C | Si | Cr | Fe | Ni |
| point 1 | 2.37 | – | 22.90 | 64.98 | 9.74 |
| point 2 | 11.04 | – | 44.11 | 40.52 | 4.33 |

*Table 4. EDS analysis of points 3 and 4 on coating 2*

| Phases | Chemical composition (wt.-%) | | | | |
|---|---|---|---|---|---|
| | C | Si | Cr | Fe | Ni |
| point 3 | 2.15 | 2.19 | 18.67 | 68.65 | 8.33 |
| point 4 | 10.72 | 0.27 | 57.23 | 30.17 | 1.61 |

composition of dendrites and interdendrite eutectics, the chemical composition of dendrites was 2.37 % C, 22.90 % Cr, 64.98 % Fe, and 9.74 % Ni, and the chemical composition of interdendrite eutectics was 11.04 % C, 44.11 % Cr, 40.52 % Fe, and 4.33 % Ni. The microstructure elements of the coating layer were distributed heterogeneously. Because of the high cooling rate in PTA coatings, and the rapid solidification of steel, there is not enough time for the elements to distribute homogeneously [23, 24]. While nickel contributes towards an austenitic solidification, chrome contributes towards the formation of interdendrite regions. The dendrites and interdendrite eutectics were composed of γ-(Fe,Ni)/$Cr_{23}C_6$ + $Cr_7C_3$ + $Fe_5C_2$ phases.

Figure 6 illustrates the SEM image for the PTA coating, produced by adding 25 % SiC (in weight) to $Cr_3C_2$. As shown in the SEM image, the density of the interdendrite eutectic increased after adding 25 % SiC. Table 4 illustrates the EDS analysis of the dendrites (point 3) and the interdendrite eutectics (point 4) as demonstrated in Figure 7. The chemical composition of point 3 was 2.15 % C, 2.19 % Si, 18.67 % Cr, 68.65 % Fe, and 8.33 % Ni, and the chemical composition of point 4 was 10.72 % C, 0.27 % Si, 57.23 % Cr, 30.17 % Fe, and 1.61 % Ni. The silicium in the microstructure proves that SiC dissolved during the coating process. Both the EDS analysis results and the XRD analysis results showed (Figure 3) that $Cr_3C_2$ and SiC dissolved in the microstructure totally. XRD analyses established that in comparison to coating 1, $Cr_3Si$ and $CrSi_2$ silicas were formed in the microstructure with the addition of SiC. Wang and Duan [25] determined $Cr_3Si$ phase in the microstructure of coating layers produced using Cr-Si-Ni powders. Zhang and Wang [26] established $Cr_3Si$ primary dendrites and $Cr_3Si/Cr_{13}Ni_5Si_2$ interdendrite eutectics in the microstructure in the conclusion of their study using Cr-Ni-Si powders.

Figure 8 shows the coating layer, interface, and substrate regions of $Cr_3C_2$ + 50 % SiC based PTA coating. As can be seen in the SEM images, planar crystallisation was observed at the interface. Cellular dendrites, columnar dendrites, and randomly oriented dendrites were found opposite the heat flux from the interface to the coating surface. Table 5 shows the results of EDS analysis of dendrites and interdendrite eutectics formed in coating 3. The chemical composition of point 5 (Figure 9) was 2.91 % C, 3.29 % Si, 18.80 % Cr, 66.58 % Fe, and 8.42 % Ni, and the chemical composition of point 6 was 9.06 % C, 0.88 % Si, 38.56 % Cr, 46.85 % Fe, and 4.65 % Ni. When compared, it is obvious that the amount of Si increased proportionally to the amount of SiC added to coating 2 and coating 3. While the amount of Si in the dendrite region of coating 2 was 2.19 %, it was found to be 3.29 % in the dendrite region of coating 3. According to coating 3 XRD analysis results, $Cr_3Si$ and $CrSi_2$ silicas were formed.

Figure 10 illustrates the SEM image of the coating produced on the surface of AISI 304 stainless steel after addition of 100 % SiC by PTA. There was a white layer between the coating layer and the substrate. This layer illustrated the excellent metallurgical bond between the coating overlay and the substrate [27]. As with the other coatings (coating 1, 2, and 3), microstructure was formed as a result of repetition of dendrites and interdendritic eutectics. Table 6 shows the results of EDS analysis of dendrites and interdendrite eutectics formed in coating 3. The chemical composition of the dendrites (point 7) was 2.68 % C, 3.61 % Si, 17.80 % Cr, 67.32 % Fe, and 8.50 % Ni, and the chemical composition of the interdendrite eutectics (point 8) was 12.91 % C, 52.11 % Cr, 33.40 % Fe, and 1.55 % Ni. Taking advantage of the data of XRD, and due to the 100 % SiC addition, these structures were $CrSi_2$ and $Fe_5SiC$ phases. As shown in Figure 11, $Fe_5SiC$ (iron silicon carbide) has a lamellar structure. $Fe_5SiC$ is an amorphous phase formed by the transformation of cementite [28].

Figure 12 depicts the change in microhardness from the coating overlay towards the substrate for coatings 1, 2, 3, and 4, produced by PTA. An increase was observed in the microhardness values recorded for the substrate towards the coating layer.

The average microhardness recorded for substrate and coating 1, 2, 3, and 4 were 200 $HV_{0.2}$, 545 $HV_{0.2}$, 592 $HV_{0.2}$, 662 $HV_{0.2}$, and 710 $HV_{0.2}$, respectively. A

| Phases | Chemical composition (wt.-%) | | | | |
|---|---|---|---|---|---|
| | C | Si | Cr | Fe | Ni |
| point 5 | 2.91 | 3.29 | 18.80 | 66.58 | 8.42 |
| point 6 | 9.06 | 0.88 | 38.56 | 46.85 | 4.65 |

*Table 5. EDS analysis of points 5 and 6 on coating 3*

| Phases | Chemical composition (wt.-%) | | | | |
|---|---|---|---|---|---|
| | C | Si | Cr | Fe | Ni |
| point 7 | 2.68 | 3.61 | 17.89 | 67.32 | 8.50 |
| point 8 | 12.95 | – | 52.11 | 33.40 | 1.55 |

*Table 6. EDS analysis of points 7 and 8 on coating 4*

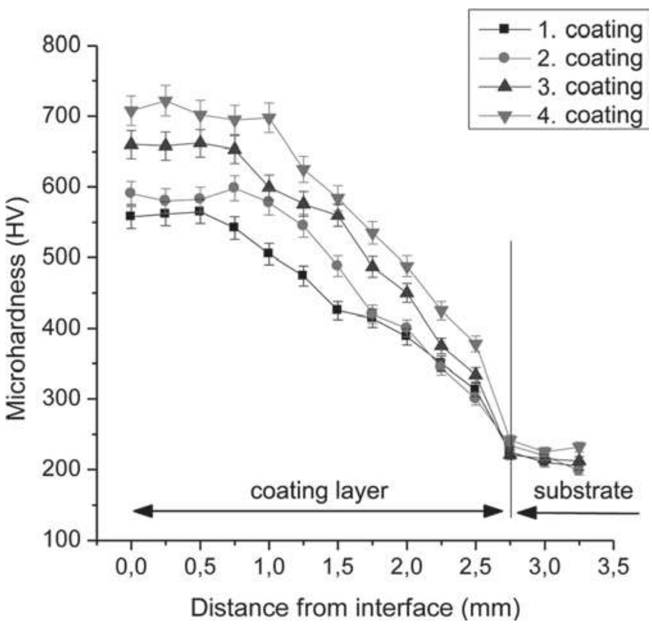


*Figure 12. The change in microhardness from the coating overlay towards the substrate*

coating layer 2.5-3.5 times harder than the substrate was obtained as a result of PTA coating. There was a significant increase in the hardness value, due to the increase in the amount of SiC in the mixture. The reasons for this change were the $CrSi_2$, $Cr_3Si$, and $Fe_5SiC$ phases in the microstructure, caused by the addition of SiC, and the microstructure change caused by rapid solidification. The formed phases displayed reinforcement element characteristics in the γ-(Fe,Ni) matrix, and caused an increase in hardness [29]. The reason for the increase in hardness from the interface towards the top section of the coating overlay was the increase in the intensity of hard phases, due to the change in cooling rates in the regions from the top section of the coating overlay towards the interface, and the shrink in size of the dendrites. This situation is associated with the fact, that the Fe content was scarce in coating area, and higher in interface area. The presence of carbide and silica phases was the reason why the hardness of the coating layer occured at different peaks [30-32].

## Conclusions

Based on the results of this investigation, the following conclusions can be drawn:

1. Homogeneous, crack-free, and nonporous $Cr_3C_2$ + SiC based coatings were formed on the surface of AISI 304 stainless steel by the plasma transferred arc (PTA) surfacing method.
2. The metallurgical bond between the coating layer and the substrate was ideal. Various shaped dendrites and interdendrite eutectics formed subject to the temperature gradient and the solidification ratio of the coating layer. According to XRD analyses, $Cr_7C_3$, $Cr_{23}C_6$, $Fe_5SiC$, $Cr_3Si$, $CrSi_2$, $Fe_5C_2$, $CFe_{15.1}$, C-(Fe,Cr)-Si, γ-(Fe,Ni), and $Fe_{0.64}Ni_{0.36}$ carbides, silicas, and complex phases were formed in the microstructure.
3. In comparison to the substrate, the microhardness of the coatings produced by PTA was 2.5-3.5 times harder. Microhardness increased with the increase of the amount of SiC added, as a result of metallographic phases, such as $CrSi_2$, $Cr_3Si$, and $Fe_5SiC$, formed in the microstructure.

## References


1 L. Zhang, D. Sun, H. Yu, H. Li: Characteristics of Fe-based alloy coating produced by plasma cladding process, Mater. Sci. Eng. A 457 (2007), pp. 319-324

2 Y. Birol: Thermal fatigue testing of Stellite 6-coated hot work tool steel, Mater. Sci. Eng. A 527 (2010), pp. 6091-6097

3 M. A. M. Silva, A. E. Martinelli, C. Alves Jr., R. M. Nascimento, M. P. Tavora, C. D. Vilar: Surface modification of Ti implants by plasma oxidation in hollow cathode discharge, Surf. Coat. Technol. 200 (2006), pp. 2618-2626

4 J. B. Cheng, B. S. Liang, X. B. Xu, Y. X. Wu: Microstructure and mechanical characteristics of iron-based coating prepared by plasma transferred arc cladding process, Mater. Sci. Eng. A 492 (2008), pp. 407-412

5 A. Gatto, E. Bassoli, M. Fornari: Plasma transferred arc deposition of powdered high performances alloys: process parameters optimization as a function of alloy and geometrical configuration, Surf. Coat. Technol. 187 (2004), pp. 265-271

6 Y. F. Liu, X. B. Liu, X. Y. Xu, S. Z. Yang: Microstructure and dry sliding wear behaviour of $Fe_2TiSi$/γ-Fe/$Ti_5Si_3$ composite coating fabricated by plasma transferred arc cladding process, Surf. Coat. Technol. 205 (2010), pp. 814-819

7 V. Balasubramanian, A. K. Lakshminarayanan, R. Varahamoorthy, S. Babu: Application of Response Surface Methodolody to Prediction of Dilution in Plasma Transferred Arc Hardfacing of Stainless Steel on Carbon Steel, J. Iron and Steel Res. Int. 16 (2009), pp. 44-53

8 P. Fan, E. Riddle, Z. Z. Fang, H. Y. Sohn: Iron aluminide coatings by an in-situ reaction process, Surf. Coat. Technol. 202 (2008), pp. 6090-6094

9 J. Wilden, J. P. Bergmann, H. Frank: Plasma transferred arc welding – modelling and experimental optimization, J. Therm. Spray Technol. 15 (2006), pp. 779-784

10 R. L. Deuis, J. M. Yellup, C. Subramanian: Metal-matrix composite coatings by PTA surfacing, Compos. Sci. Technol. 58 (1998), pp. 299-309

11 M. Li, H. He, G. Sun: Laser cladding Co-based alloy/SiC(P) composite coatings on IF steel, Mater. Des. 25 (2004), pp. 355-358

12 H. O. Pierson: Handbook of refractory carbides and nitrides: Properties, characteristics, processing and applications, Noyes Publications, Westwood, New Jersey (1996)

13 Z. Dawei, T. Li, T. C. Lei: Laser cladding of Ni-$Cr_3C_2$/(Ni + Cr) composite coating, Surf. Coat. Technol. 110 (1998), pp. 81-85

14 C. Sudha, P. Shankar, R. V. Subba Rao, R. Thirumurugesan, M. Vijayalakshmi, B. Raj: Microchemical and microstructural studies in a PTA weld overlay of Ni-Cr-Si-B alloy on AISI 304L stainless steel, Surf. Coat. Technol. 202 (2008), pp. 2103-2112

15 Z. Huang, Q. Hou, P. Wang: Microstructure and properties of $Cr_3C_2$-modified nickel-based alloy coating deposited by plasma transferred arc process, Surf. Coat. Technol. 202 (2008), pp. 2993-2999

16 S. Buytoz, M. Ulutan: In situ synthesis of SiC reinforced MMC surface on AISI 304 stainless steel by TIG surface alloying, Surf. Coat. Technol. 200 (2006), pp. 3698-3704

17 M. Guo, A. Liu, M. Zhao, H. Hu, Z. Wang: Microstructure and wear resistance of low carbon steel surface strengthened by plasma melt injection of SiC particles, Surf. Coat. Technol. 202 (2008), pp. 4041-4046

18 G. Thawari, G. Sundarararjan, S. V. Joshi: Laser Surface Alloying of Medium Carbon Steel with SiC(P), Thin Solid Films 423 (2003), pp. 41-43

19 A. Hidouci, J. M. Pelletier, F. Ducoin, D. Dezert, R. E. Guerjouma: Microstructural and mechanical characteristics of laser coatings, Surf. Coat. Technol. 123 (2000), pp. 17-23

20 Q. Li, T. C. Lei, W. Z. Chen: Microstructural characterization of WCp reinforced Ni-Cr-B-Si-C


## Abstract


**Charakterisierung der Mikrostruktur und Mikrohärte von $Cr_3C_2$-SiC PTA-Beschichtungen.** Das Ziel der hier beschriebenen Arbeiten bestand darin die $Cr_3C_2$- und SiC-Pulverbeschichtungen zu untersuchen, die mittels eines Plasmalichtbogenprozesses auf Stahl AISI 304 aufgebracht wurden. Der SiC-Gehalt der so produzierten Schicht wurde zwischen 0 wt.-% und 100 wt.-% variiert und der Effekt der SiC-Konzentration auf die Mikrostruktur und Härte der Beschichtungen wurde experimentell bestimmt. Mittels REM-Untersuchungen wurde ermittelt, dass die Kompositbeschichtungen eine homogene, porenfreie und rissfreie Mikrostruktur aufwiesen. Dendrit- und Interdendrit-Eutektika bildeten sich auf der Schicht abhängig vom Verhältnis aus Temperaturgradienten und Erstarrungsgeschwindigkeit. Es konnte ein signifikanter Härteanstieg in den Schichten aufgrund des Effektes der in der Mikrostruktur gebildeten Phasen γ-(Fe,Ni), $Cr_7C_3$, $Cr_{23}C_6$, $Fe_5C_2$, $Cr_3Si$, $CrSi_2$, $Fe_{0.64}Ni_{0.36}$, $CFe_{15.1}$, C-(Fe,Cr)-Si festgestellt werden. Im Vergleich zum Substrat war die Mikrohärte in den mit PTA produzierten Schichten 2,5-3,5 mal härter.

composite coatings, Surf. Coat. Technol. 114 (1999), pp. 285-291

21 C. T. Kwok, F. T. Cheng, H. C. Man: Laser surface modification of UNS S31603 stainless steel. Part I: microstructures and corrosion characteristics, Mater. Sci. Eng. A 290 (2000), pp. 55-73

22 J. S. Selvan, K. Subramanian, A. K. Nath, H. Kumar, C. Ramachandra, S. P. Ravindranathan: Laser boronising of Ti-6Al-4V as a result of laser alloying with pre-placed BN, Mater. Sci. Eng. A 260 (1999), pp. 178-187

23 Q. Y. Hou, Z. Huang, J. T. Wang: Influence of nano-$Al_2O_3$ particles on the microstructure and wear resistance of the nickel-based alloy coating deposited by plasma transferred arc overlay welding, Surf. Coat. Technol. 205 (2011), pp. 2806-2812

24 A. Conde, R. Colaco, R. Vilar, J. Damborenea: Corrosion behaviour of steels after laser surface melting, Mater. Des. 21 (2000), pp. 441-445

25 H. M. Wang, G. Duan: Microstructure and wear resistance of a laser clad reinforced $Cr_3Si$ metal silicide composite coating, Mater. Sci. Eng. A 336 (2002), pp. 117-123

26 L. Q. Zhang, H. M. Wang: High-temperature sliding wear resistance of a $Cr_3Si/Cr_{13}Ni_5Si_2$ multiphase intermetallic alloy, Mater. Lett. 57 (2003), pp. 2710-2715

27 S. Buytoz: Microstructural properties of M7C3 eutectic carbides in a Fe-Cr-C alloy, Mater. Lett. 60 (2006), pp. 605-608

28 A. V. Syugaev, S. F. Lomaewa, A. N. Maratkanova, D. V. Surnin, S. M. Reshetnikov: Electrochemical Properties of Iron Silicocarbide and Cementite in Acidic and Neutral Environments, Prot. Met. Phys. Chem. Surf. 45 (2009), pp. 81-88

29 H. M. Wang, G. Duan: Wear and corrosion behaviour of laser clad $Cr_3Si$ reinforced intermetallic composite coatings, Intermetallics 11 (2003), pp. 755-762

30 X. Guozhi, Z. Dongjie, W. Yuping, L. Pinghua: Microstructure and corrosion properties of thick WC composite coating formed by plasma cladding, Appl. Surf. Sci. 256 (2010), pp. 6354-6358

31 G. Xu, M. Kutsuna, Z. Liu, H. Zhang: Characteristics of Ni-based coating layer formed by laser and plasma cladding processes, Mater. Sci. Eng. A 417 (2006), pp. 63-72

32 Y. C. Lin, Y. C. Lin: Elucidation of microstructure and wear behaviours of Ti–6Al–4V cladding using tungsten boride powder by the GTAW method, J. Coat. Technol. Res. 8 (2011), pp. 247-253

## The Authors of This Contribution

Dr. Serkan Islak graduated from Metallurgy Education Department in Firat University, Elazig, Turkey, in 2002. He holds M.Sc. and Ph.D. at Firat University, Elazig, in 2005 and 2012, respectively. He is instructor at the Cide Rifat Ilgaz Vocational High School, Welding Technology Department of Kastamonu University, Kastamonu, Turkey. His main interests include powder metallurgy and surface coating technologies.

Dr. Ozkan Eski graduated from Mechanical Engineering Department in Istanbul Technical University, Istanbul, Turkey, in 1989. He holds M.Sc. and Ph.D. at Istanbul Technical University, Istanbul, in 1993 and 2001, respectively. He is assistant professor at Kastamonu Vocational High School, Mechanical Department of Kastamonu University, Kastamonu, Turkey. His main interests include welding technologies.

Dr. Soner Buytoz graduated from Mechanical Engineering in Firat University, Elazig, Turkey, in 1996. He holds M.Sc. and Ph.D. at Firat University, Elazig, in 1999 and 2004, respectively. He is assistant professor at the Department of Metallurgy and Materials Engineering, Technology Faculty, Firat University, Elazig, Turkey. His main interests include surface coating and abrasion wear of materials, composite materials and their mechanical behaviour as well as corrosion.

Muzaffer Karagoz graduated from Mechanical Engineering in Eskisehir Osmangazi University, Eskisehir, Turkey, in 2005. He holds M.Sc. at Eskisehir Osmangazi University, Eskisehir, Turkey in 2010. He is research assistant in Engineering Faculty, Department of Metallurgical and Materials Engineering, Bartin, Turkey. His main interests include manufacturing technologies.

Dr. Joseph Stokes graduated from Mechanical and Manufacturing Engineering from Trinity College Dublin, Ireland in 1997. He holds Ph.D. at Dublin City University in 2003, Dublin, Ireland. He lectured part-time for two years in Dublin Institute of Technology Bolton Street from 1998 to 2000. In September 2000 he became a member of the academic staff in the School of Mechanical and Manufacturing Engineering in Dublin City University, Ireland. He was promoted to position of senior lecturer in DCU in 2009. He has been research active in the area of surface engineering since 1997. Applications of his research include: wear reduction, bio-coatings for implant replacement therapy, oil and gas protective coatings to mention a few.

You will find the article and additional material by entering the document number MP110397 on our website at www.materialstesting.de